Symmetry-resolved density of states from valence band photoelectron diffraction

Ch. Søndergaard and Ch. Schultz
Institute for Storage Ring Facilities, University of Aarhus, DK-8000 Aarhus C, Denmark

M. Schønning
Institute for Physics and Astronomy and CAMP, University of Aarhus, DK-8000 Aarhus C, Denmark

S. Lizzit
Sincrotrone Trieste S.C.p.A., s.s. 14 Km 163.5, 34012 Trieste, Italy

A. Baraldi
Sincrotrone Trieste S.C.p.A., s.s. 14 Km 163.5, 34012 Trieste and Dipartimento di Fisica, Università di Trieste, Via Valerio 2, 34127 Trieste, Italy
and Laboratorio TASC-INFM, Padriciano 99, 34012 Trieste, Italy

S. Agergaard and M. B. Nielsen
Institute for Storage Ring Facilities, University of Aarhus, DK-8000 Aarhus C, Denmark

H. Li
Institute for Storage Ring Facilities, University of Aarhus, DK-8000 Aarhus C, Denmark
and Department of Physics, Zhejiang University, Hangzhou 310027, China

Ph. Hofmann
Institute for Storage Ring Facilities, University of Aarhus, DK-8000 Aarhus C, Denmark
(Received 4 July 2001; published 6 December 2001)

We suggest that valence band photoelectron diffraction can be used to decompose a solid's density of states (DOS) into components of different symmetry. This approach is illustrated by breaking down the density of states of aluminum into its *s* and *p* components. The results reveal a more *s*-like DOS at the bottom of the band and a more *p*-like DOS near the Fermi level, in qualitative agreement with calculations. A quantitative comparison does, however, show that the measured DOS contributions are narrower, i.e., more ''atomiclike'' than the calculated ones. Possible reasons are discussed.

DOI: 10.1103/PhysRevB.64.245110 PACS number(s): 71.20.−b, 79.60.−i

Understanding the electronic structure of new and complex materials is a major challenge in current solid-state physics. The electronic states very close to the Fermi level are of particular interest because they are responsible for a large number of phenomena: metal-insulator transitions, high-T_c superconductivity, and magnetoresistance. A promising approach for measuring the density of states (DOS) of complex materials is soft x-ray fluorescence spectroscopy.[1] This technique offers the possibility to determine chemically resolved and symmetry-restricted partial densities of states (PDOS) if a suitable core level is available. In this paper, we discuss valence band photoelectron diffraction (VBPED) as an alternative method which potentially combines the possibility of higher spectral resolution with stringent symmetry restrictions. We use this technique to break down the density of states of aluminum into the *s* and *p* contributions.

Photoelectron diffraction (PED) is an effect known from core-level spectroscopy: The photoelectron wave undergoes a multiple-scattering process at the neighbors of the emitting atom such that modulations of the measured photoemission intensity are observed as a function of emission angle or electron kinetic energy.[2] At high photon energies and/or high temperatures the valence band shows the same PED modulations as the core levels[3,4] even though the initial-state wave function is delocalized. The reason is an effective localization which could either be ''real''[3] or caused by an integration over all initial states in momentum space.[4–6] Recently, Stuck and co-workers have shown that this valence band photoelectron-diffraction effect can be used to extract the chemically resolved PDOS of an alloy, Cu_3Au.[7,8]

Using VBPED to determine the symmetry-resolved PDOS is more difficult because of the small effect that the initial-state symmetry has on the diffraction pattern. While evidence for such an influence has been reported for transition metals,[4,9,10] a systematic decomposition has not been attempted up to now, to the best of our knowledge. Here the *s* and *p* PDOS contributions of aluminum are determined by comparing the energy-resolved VBPED modulations to the PED modulations of the Al 2*s* and 2*p* core levels *taken at the same kinetic energy* and thus under the same scattering conditions. Aluminum is a good test candidate because its quasi-free-electron character renders it a ''worst case'' example for the experiment. If the decomposition works on Al it will most probably also work on materials with more localized bonding.

The Al(001) sample was prepared by cycles of Ar ion sputtering and annealing. This resulted in a sharp (1×1)

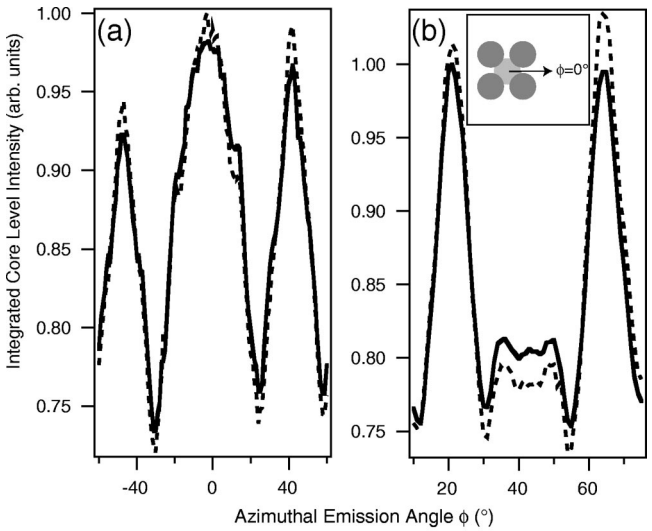

FIG. 1. (a) Integrated intensity of the Al 2*s* (dashed) and 2*p* (solid) core levels for an azimuthal scan 35° off normal with a kinetic energy of about 400 eV. The curves have been multiplied by an arbitrary factor in order to permit a better comparison. (b) The same but for 56° off normal with a kinetic energy of about 350 eV. Inset: definition of the azimuthal angle scale.

low-energy electron-diffraction pattern and a contamination level below the limit of x-ray photoelectron spectroscopy. The data were taken at the SuperESCA beamline at the synchrotron light source ELETTRA. The experimental geometry is such that the electron energy analyzer is mounted 40° away from the incoming light, in the plane of polarization. All data shown here are so-called azimuthal scans: the polar emission angle Θ was kept fixed and the photoemission intensity for the core levels and the valence band was measured as a function of the azimuthal emission angle ϕ. The zero of the azimuthal scale is defined in Fig. 1. Note that the azimuthal scans should be symmetric around $\phi=0°$ because of a mirror plane in the crystal. Two data sets consisting of several core-level and one valence band azimuthal scan have been taken, one at a kinetic energy of about 400 eV and at $\Theta=35°$ away from the surface normal (called set I in the following), the other at a kinetic energy of about 350 eV, at $\Theta=56°$ off normal (set II). Both were taken at a sample temperature of 673 K. Choosing such a high temperature is a convenient way to suppress the contribution of the direct, $\vec{k}$ conserving, transitions to the valence band spectra.[4] Valence band azimuthal scans were also taken at lower energies and lower temperatures in order to investigate the effect of the direct transitions.

Figure 1(a) shows the result of the Al 2*s* and 2*p* azimuthal angle scans for data set I, i.e., at $\Theta=35°$ off normal and a kinetic energy of about 400 eV. For the sake of comparison the curves have been multiplied by an arbitrary factor. Two main features are observed in the data. The peaks at $\phi=\pm45°$ are the shoulders of a pronounced forward-scattering peak which appears in the [101]-like crystallographic directions of the face-centered-cubic structure, i.e., for a situation where $\Theta=\phi=45°$. The peak at $\phi=0°$ is close to the bulk [112] direction. Note, however, that in this energy range multiple scattering is important and the PED patterns cannot be understood simply by considering the crystallographic directions. The modulations of the *s* and *p* core levels are rather similar. There are, however, some small but well-reproducible differences, the most important being the stronger modulation of the *s* core level. Another difference is the smaller relative intensity of the shoulders at the sides of the $\phi=0°$ peak for the *s* core level. Figure 1(b) shows the same for data set II. As in the first data set, the *s* component shows a somewhat stronger degree of modulation. It also has a smaller intensity around $\phi=45°$, i.e., at the center of the scan. The same behavior and nearly the same results can also be found in simulated data sets obtained using the MSCD package.[11]

In Fig. 2 the result of the corresponding scans of the valence band are given. The left-hand side of the figure shows the raw data. Every column of the displayed matrix corresponds to an energy distribution curve (EDC). The black area at the top is due to the cutoff character of the Fermi function. Below the Fermi edge the intensity is decreasing until the bottom of the band is reached. At the lowest kinetic energies the intensity is increasing again due to the surface-plasmon losses associated with the photoemission from the valence band. The VBPED is already visible in the raw data but it emerges much more clearly in the modulation function shown on the right-hand side of Fig. 2. This modulation function is formed for each row of constant kinetic energy by taking $[I(\phi)-I_0]/I_0$ where $I(\phi)$ is the measured intensity and I_0 is the average of $I(\phi)$. Above the Fermi level this normalization procedure results in intense noise because of the fact that I_0 has values very close to zero. In the valence band data for set I as given in Fig. 2(a) one easily recognizes the three main peaks already seen in the core-level data. A closer inspection reveals that the VBPED signal depends on the binding energy: at the bottom of the valence band, from about 11 eV to 6 eV below the Fermi level, the modulation is stronger (i.e., the maxima are higher) and the shoulders of the $\phi=0°$ peak are smaller. When comparing this to the core-level data it qualitatively suggests that the bottom of the band is more *s* like than the top of the band. For data set II in Fig. 2(b) the energy dependence seems less pronounced. At the bottom of the band the intensity around $\phi=40°$ is a little smaller, also indicative of *s*-like states and in the immediate vicinity of the Fermi level the total modulation is stronger, unlike in data set I.

For a more quantitative analysis it is necessary to consider the intensities of the valence band and the core levels rather than the modulation functions. We follow a procedure outlined by Stuck *et al.* for the decomposition of the valence band of Cu_3Au into the copper and gold contributions.[7] Assuming that the final-state diffraction for the *s* and *p* parts of the valence band are exactly the same as for the corresponding core levels, we write the energy-resolved valence band intensity $I^{VB}(\phi,E)$ as a sum over the integrated core-level intensities $S_s^{core}(\phi)$ and $S_p^{core}(\phi)$,

$$I^{VB}(\phi,E)=\sum_{i=s,p} S_i^{core}(\phi)c_i d_i^{VB}(E). \qquad (1)$$

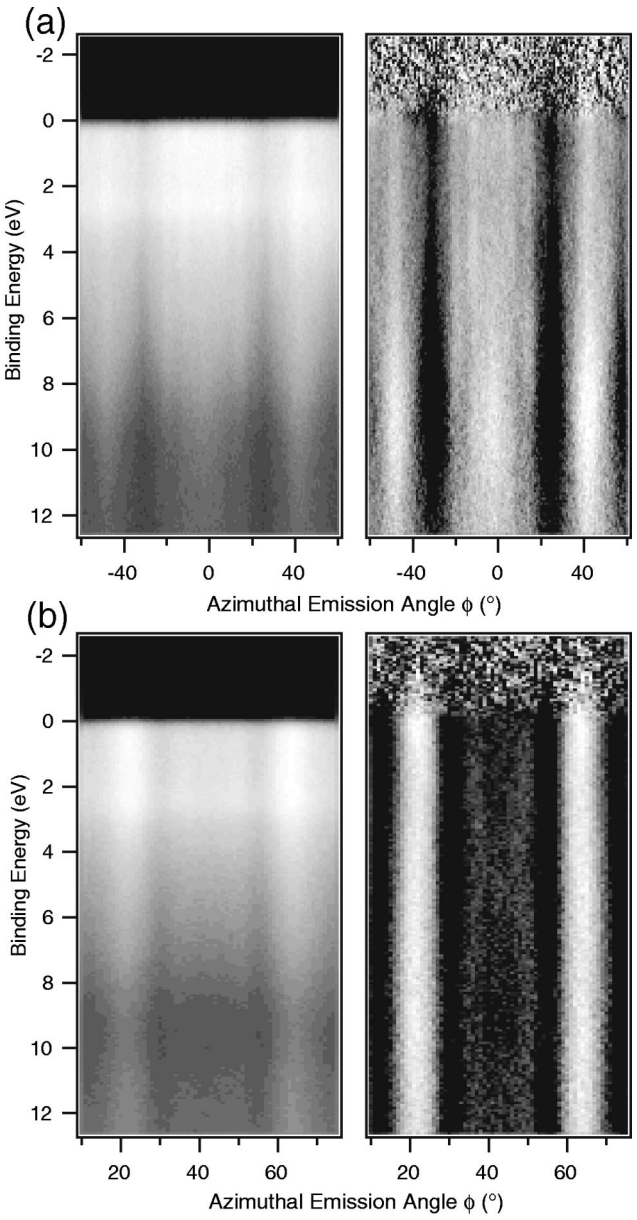

FIG. 2. (a) Photoemission intensity from a valence band scan corresponding to Fig. 1(a). The lowest values are black, the highest white. Left: raw data. Right: modulation function $[I(\phi)-I_0]/I_0$ calculated for each kinetic energy. (b) The same, corresponding to Fig. 1(b).

The factors c_i contain cross sections which are assumed to be independent of ϕ and E as well as the number of electrons in the s and p states. $d_i^{VB}(E)$ is the PDOS. In practice, the decomposition is achieved by finding the factors $d_i^{VB}(E)$ such that the right side of the equation represents the best fit to the left side for every kinetic energy. If the values of the c_i are unknown, this procedure results in the PDOS for the s and p states on an arbitrary scale. We have determined the core-level intensities $S_i^{core}(\phi)$ in Fig. 1 using a fit with a Shirley-type background. When comparing the core-level scans to the valence band, one has to take into account the large width of the latter and the possibility of changing diffraction conditions in this energy range. We have therefore

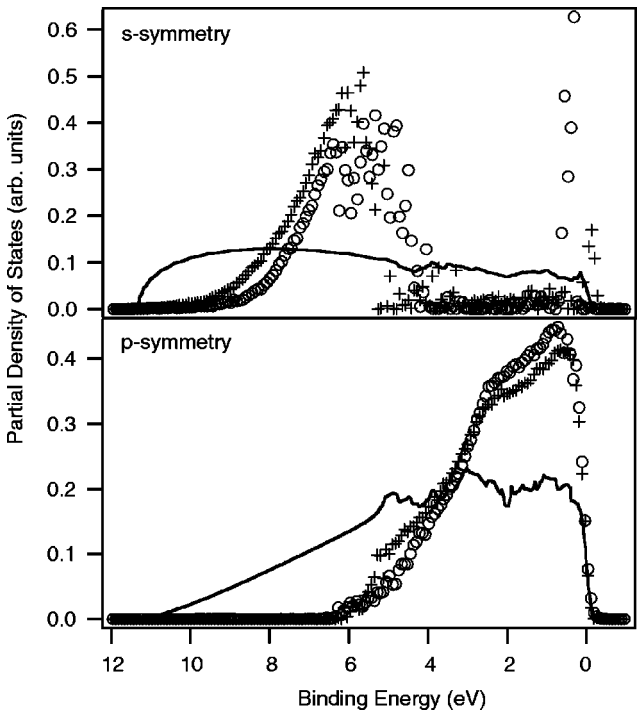

FIG. 3. Partial s and p density of states for Al obtained from comparing the valence band data in Figs. 2(a) and 2(b) to the corresponding core-level data. Crosses: result from the scans taken at 35° off normal with a kinetic energy of about 400 eV; open circles: from 56° off normal with a kinetic energy of about 350 eV. Solid lines: calculated PDOS after Ref. 12, convoluted with a Fermi distribution.

taken core-level scans at three different kinetic energies spanning the valence band region and interpolated the intensity in between. The energy-resolved valence band intensity $I^{VB}(\phi,E)$ was obtained by subtracting a Shirley-type background from the raw data.

The result of the decomposition is given in Fig. 3. The resulting PDOS components for both data sets are plotted together with the theoretical PDOS,[12] cut off by a Fermi distribution. Each set of curves is normalized such that the area under the experimental curves is the same as under the calculated curve. The theoretical PDOS was obtained by means of *ab initio* density-functional calculations using the local-density approximation. The self-consistent solution of the one-electron Schrödinger-like equation was obtained by means of the linear muffin-tin orbital method in the so-called atomic spheres approximation.[13] Apart from the s and p components, a decomposition of the theoretical DOS also yields a small d component in the upper part of the band and a very small f component. The relative contribution of these components is, however, small enough with respect to the precision we aim for here. The valence band DOS is split in two regions: the bottom of the band is more s like and the top of the band is more p like, in accordance with naive intuition and the visual inspection of Fig. 2. This ordering is also found in the theoretical prediction (also plotted in Fig. 3) but our PDOS contributions are more ''atomiclike,'' i.e., the s and p components are narrower. Note that the result is very similar for both data sets even though they correspond to

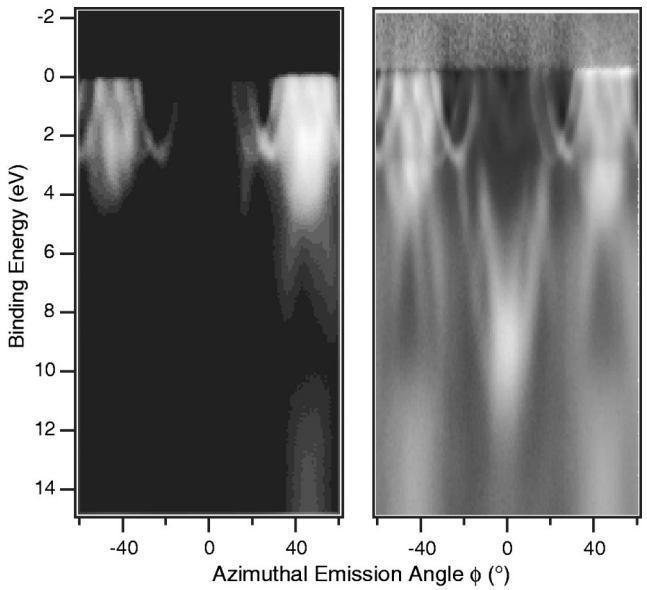

FIG. 4. Azimuthal scan of the valence band taken at 45° off normal and a sample temperature of 128 K. Left: raw data. Right: modulation function. The direct transitions are visible as narrow and strongly dispersing features.

rather different scattering conditions. The sharp spike in the *s* PDOS from data set II is caused by the strong modulation at this binding energy which can be observed in Fig. 2(b). Its physical origin is, however, unclear.

Before discussing reasons for the difference between experiment and theory we would like to address the possible sources of error in this way of analyzing the data. The first problem is purely statistical: the difference between the *s* and *p* core-level scans is clear but it is small. Note that this difference could be increased by changing the experimental geometry. Indeed, it might be possible to decompose the *s* and *p* contributions to the valence band by taking data in two different geometries, one where the photoemission intensity of the *s* states is exactly zero and one where it is not.[14]

The fact that we obtain similar results for both data sets, however, suggests that the statistical errors may be only a minor problem and we have to examine the sources of systematic error. The first is the possible residual intensity of direct transitions. These are suppressed by the high temperature and the high photon energy but they could still represent a problem in view of the small difference between *s* and *p* scattering. We have therefore performed detailed studies of the direct-transition intensity as a function of photon energy and temperature from which we can conclude that the remaining direct-transition intensity is of no significance here.[15] Note also that direct transitions appear as sharp structures in plots like Fig. 2 and would be easily recognized. This is illustrated in Fig. 4 which shows an azimuthal scan of the valence band taken at $\Theta = 45°$ off normal, a kinetic energy of about 194 eV and 128 K. The low photon energy and low temperature increase the intensity of the direct transitions. They are clearly observed in the raw data and even better in the modulation function. In view of these arguments and data, we exclude direct transitions as a major source of systematic error here.

The next possible source of error is the background in the valence band data. The background might show modulations similar to the actual photoemission intensity, depending on its nature (intrinsic or extrinsic). It is well established that such modulations are present in the losses from core-level data[16] and also in Fig. 1 modulations are evident below the bottom of the band, in the region of the surface-plasmon loss. Note that the subtraction of the Shirley background from each EDC in the valence band data does, to some extent, take care of this problem.

Another questionable point is our assumption that the initial-state-dependent modulations of the valence band are exactly the same as those of the corresponding core-levels. The possible problem here is that the initial-state symmetry of a fully occupied core level is different from a partially filled valence band state and this can lead to different diffraction effects.[10,17] We do not think that this is a severe problem here due to the high symmetry of the crystal.

Finally, we have identified the $d_i^{VB}(E)$ directly with the PDOS. This is only approximately correct since the $d_i^{VB}(E)$ might have a directional dependence.[7] First of all, the dipole selection rules only allow transitions from certain initial states, although this condition will be relaxed by the interaction with phonons. A more severe reason for the directional dependence could be the fact that the ratio between the contribution of surface and bulk PDOS to the measured signal will change strongly as a function of the polar emission angle. This point is discussed below.

After these words of caution we can now come back to the question of why there are differences between our experimental PDOS and the theoretical prediction. We have two possible explanations. The first is that the measured PDOS is a superposition of surface and bulk PDOS. In general one expects a band narrowing at the surface which changes the shape of the occupied PDOS. In the particular case of Al(001) the Shockley-type surface state at the $\bar{\Gamma}$ point of the surface Brillouin zone plays an important role. This surface state is situated in the bulk band gap near the *X* point. It is located very close to the band edge and penetrates deeply into the bulk. The surface state is considerably increasing the local density of states in the first layers. In order to keep charge neutrality, this is compensated for by an overall band narrowing,[18] consistent with our observations. A comparison between photoemission experiments on Al(001) at low photon energies and the calculated electronic structure has also led to the conclusion that the local density of states at the surface of Al(001) is dominated by the surface state.[19] If the changes of the PDOS at the surface were indeed responsible for our results, one would in principle expect this effect to be stronger for data set I than for data set II because of the higher polar emission angle and the lower photon energy. In the case of a deeply penetrating surface state, however, this difference would be small. The real importance of the surface PDOS contributions could be checked by a calculation of the layer-resolved PDOS of Al(001).

Another possible explanation is that the reason lies in the measurement itself. Consider a picture where, for whatever reason, the electrons which give rise to the VBPED effect can be viewed as locally emitted from near the atom cores. In

such a case the VBPED experiment would primarily probe the wave functions near the core and the resulting PDOS would probably be more atomiclike than the total PDOS. It is clear that this ''artificial'' band narrowing would be stronger on our free-electron-like metal Al than on *d* and *f* systems where the initial state is already rather localized.

In conclusion, we have shown that VBPED can be used to decompose the DOS of a solid into contributions of different initial-state angular momenta (symmetry), even in the case of a free-electron-like metal. We get rather similar results from data sets taken under different scattering conditions. They show the right ordering of the *s* and *p* dominated regions in the DOS but the quantitative comparison with the calculated DOS is unsatisfactory. An experimental approach to solving this problem could be to attempt a similar experiment on an apparatus where the polarization conditions of the light can be chosen such that the difference between *s* and *p* becomes much bigger. However, the similar results from the two sets of data presented in the present work make it likely that the problem lies less with the experiment than with the interpretation of the result. Note that we achieve the decomposition by a comparison to measured core-level data. Alternatively, one could compare to calculated symmetry-resolved modulations which would remove the problem of having to compare the valence band data to a core level with a different main quantum number. In the future, VBPED could complement x-ray fluorescence experiments, in particular in the case of investigations where high spectral resolution and symmetry restriction is required, but the fundamental physics behind the technique is still not completely understood.

The authors gratefully acknowledge stimulating discussions with N.E. Christensen, T. Greber, J. Osterwalder, G. Zampieri, and E.W. Plummer. H. Li thanks the Danish Foreign Ministry for financial support. This project was supported by the Danish National Research Council and the European Union.

[1] J.A. Carlisle, E.L. Shirley, L.J. Terminello, J.J. Jia, T.A. Callcott, D.L. Ederer, R.C.C. Perera, and F.J. Himpsel, Phys. Rev. B **59**, 7433 (1999), and references therein.

[2] D.P. Woodruff, in *Angle-Resolved Photoemission, Theory and Current Applications*, edited by S.D. Kevan (Elsevier, Amsterdam, 1992).

[3] J. Osterwalder, T. Greber, S. Hüfner, and L. Schlapbach, Phys. Rev. Lett. **64**, 2683 (1990).

[4] G.S. Herman, T.T. Tran, K. Higashiyama, and C.S. Fadley, Phys. Rev. Lett. **68**, 1204 (1992).

[5] D.D. Sarma, W. Speier, and J.F.v. Acker, Phys. Rev. Lett. **66**, 2834 (1991).

[6] M.A. Vincente Alvarez, H. Ascolani, and G. Zampieri, Phys. Rev. B **54**, 14 703 (1996).

[7] A. Stuck, J. Osterwalder, T. Greber, S. Hüfner, and L. Schlapbach, Phys. Rev. Lett. **65**, 3029 (1990).

[8] A. Stuck, J. Osterwalder, T. Greber, L. Schlapbach, R.C. Albers, and M. Alouani, Phys. Rev. B **51**, 9497 (1995).

[9] L.E. Klebanoff, and D.G.V. Campen, Phys. Rev. Lett. **69**, 196 (1992).

[10] K.T. Park, M. Richards-Babb, J.S. Hess, J. Weiss, and K. Klier, Phys. Rev. B **54**, 5471 (1996).

[11] Yufeng Chen and Michel A. Van Hove, World Wide Web site http://electron.lbl.gov/mscdpack/

[12] N. E. Christensen (private communication).

[13] O.K. Andersen, Phys. Rev. B **12**, 3060 (1975).

[14] T. Greber and A. Morgante (private communication).

[15] Ch. Søndergaard, Ph. Hofmann, Ch. Schultz, M.S. Moreno, J.E. Gayone, M.A. Vicente Alvarez, G. Zampieri, S. Lizzit, and A. Baraldi, Phys. Rev. B **63**, 233102 (2001).

[16] E.J. Moler, S.A. Kellar, Z. Hussain, Y. Chen, D.A. Shirley, W.R.A. Huff, and Z. Huang, Phys. Rev. B **56**, 16 016 (1997).

[17] J. Osterwalder, T. Greber, P. Aebi, R. Fasel, and L. Schlapbach, Phys. Rev. B **53**, 10 209 (1996).

[18] J.E. Inglesfield and G.A. Benesh, Surf. Sci. **200**, 135 (1988).

[19] C. Stampfl, K. Kambe, R. Fasel, P. Aebi, and M. Scheffler, Phys. Rev. B **57**, 15 251 (1998).